Brain, Behavior, and Immunity 65 (2017) 350–361

Contents lists available at ScienceDirect

Brain, Behavior, and Immunity

journal homepage: www.elsevier.com/locate/ybrbi

Full-length Article

Cathepsin B plays a critical role in inducing Alzheimer's disease-like phenotypes following chronic systemic exposure to lipopolysaccharide from *Porphyromonas gingivalis* in mice

Zhou Wu [a,b,*,1], Junjun Ni [a,1], Yicong Liu [a], Jessica L. Teeling [c], Fumiko Takayama [a], Alex Collcutt [c], Paul Ibbett [c], Hiroshi Nakanishi [a]

[a] Department of Aging Science and Pharmacology, Kyushu University, Japan
[b] OBT Research Center, Faculty of Dental Science, Kyushu University, Japan
[c] Biological Sciences, Faculty of Natural and Environmental Sciences, University of Southampton, United Kingdom

ARTICLE INFO

Article history:
Received 19 August 2016
Received in revised form 5 June 2017
Accepted 6 June 2017
Available online 10 June 2017

Keywords:
Lipopolysaccharide from *Porphyromonas gingivalis*
Middle age
Cathepsin B
Microglia
Neuroinflammation
Intracellular amyloid beta accumulation
Alzheimer's disease

ABSTRACT

A number of clinical and experimental studies have revealed a strong association between periodontitis and accelerated cognitive decline in Alzheimer's disease (AD); however, the mechanism of the association is unknown. In the present study, we tested the hypothesis that cathepsin (Cat) B plays a critical role in the initiation of neuroinflammation and neural dysfunction following chronic systemic exposure to lipopolysaccharide from *Porphyromonas gingivalis* (PgLPS) in mice (1 mg/kg, daily, intraperitoneally). Young (2 months old) and middle-aged (12 months old) wild-type (WT; C57BL/6N) or CatB-deficient (*CatB*$^{-/-}$) mice were exposed to PgLPS daily for 5 consecutive weeks. The learning and memory function were assessed using the passive avoidance test, and the expression of amyloid precursor protein (APP), CatB, TLR2 and IL-1β was analyzed in brain tissues by immunohistochemistry and Western blotting. We found that chronic systemic exposure to PgLPS for five consecutive weeks induced learning and memory deficits with the intracellular accumulation of Aβ in neurons in the middle-aged WT mice, but not in young WT or middle-aged *CatB*$^{-/-}$ mice. PgLPS significantly increased the expression of CatB in both microglia and neurons in middle-aged WT mice, while increased expression of mature IL-1β and TLR2 was restricted to microglia in the hippocampus of middle-aged WT mice, but not in that of the middle-aged *CatB*$^{-/-}$ ones. In *in vitro* studies, PgLPS (1 μg/ml) stimulation upregulated the mean mRNA expression of IL-1β, TLR2 and downregulated the protein levels of IκBα in the cultured MG6 microglia as well as in the primary microglia from WT mice, which were significantly inhibited by the CatB-specific inhibitor CA-074Me as well as by the primary microglia from *CatB*$^{-/-}$ mice. Furthermore, the mean mRNA expression of APP and CatB were significantly increased in the primary cultured hippocampal neurons after treatment with conditioned medium from PgLPS-treated WT primary microglia, but not after treatment with conditioned medium neutralized with anti-IL-1beta, and not after treatment with conditioned medium from PgLPS-treated *CatB*$^{-/-}$ primary microglia or with PgLPS directly. Taken together, these findings indicate that chronic systemic exposure to PgLPS induces AD-like phenotypes, including microglia-mediated neuroinflammation, intracellular Aβ accumulation in neurons and impairment of the learning and memory functions in the middle-aged mice in a CatB-dependent manner. We propose that CatB may be a therapeutic target for preventing periodontitis-associated cognitive decline in AD.

1. Introduction

Alzheimer's disease (AD), the most common cause of dementia, is a major health problem in aging societies worldwide (Blennow et al., 2006). AD is characterized by three major histopathological hallmarks: β-amyloid (Aβ) plaques, neurofibrillary tangles and microglia-mediated neuroinflammation. Growing evidence suggests that microglia play a key role in the pathogenesis of AD (Edison et al., 2008; McGeer and McGeer, 2010; Okello et al., 2009; Wyss-Coray, 2006), by promoting neuroinflammation, Aβ deposition and neuronal dysfunction (Kahn et al., 2012; Streit et al., 2004). Histological evidence confirms that Aβ senile plaques

* Corresponding author.
E-mail address: zhouw@dent.kyushu-u.ac.jp (Z. Wu).
[1] Zhou Wu and Junjun Ni contributed equally to this work.

http://dx.doi.org/10.1016/j.bbi.2017.06.002
0889-1591/

are associated with activated microglia, which are immune-positive for pro-inflammatory cytokines, including IL-1β (Shaftel et al., 2008; Wu et al., 2013a). Neuroinflammation has been implicated as a contributor to the pathogenesis of AD (Hickman et al., 2008), and anti-inflammatory agents lower the risk of AD by dampening neuroinflammation (Vlad and Donald, 2008).

Systemic inflammation exacerbates age-dependent microglia-mediated neuroinflammation via the increased production of pro-inflammatory cytokines (Perry, 2004; Perry et al., 2003; Wu et al., 2008, 2013). In addition, repeat injections of high-dose lipopolysaccharide from *Escherichia coli* have been reported to induce amyloid deposition, hyper-phosphorylation of tau and memory deficits in wild-type (WT) mice, and we have found that chronic systemic inflammation induces deficits in the hippocampal LTP in middle-aged rats through microglia-mediated neuroinflammation (Liu et al., 2012). These observations imply that microglia-mediated neuroinflammation following chronic systemic inflammation drives the onset and progression of the pathological hallmarks and clinical symptoms of AD.

Periodontitis, the most common oral chronic multi-bacterial infection, induces and amplifies low-grade systemic inflammation resulting from the relevant bacteria and their components entering the body through the systemic circulation. (Pischon et al., 2007). Periodontitis has been identified as a risk factor for progression of AD (Ide et al., 2016; Kamer et al., 2008; Noble et al., 2009). However, the mechanism underlying this association is unknown. The major periodontal bacteria is *Porphyromonas gingivalis* (Pg), and its lipopolysaccharide (PgLPS) has been detected in the brains of AD patients (Poole et al., 2013). We recently found that PgLPS induces the activation of leptomeninges/choroid plexus, which is formed at the blood-cerebrospinal fluid barrier (BCSFB), resulting in the induction of microglia-mediated neuroinflammation (Liu et al., 2013; Wu and Nakanishi, 2015).

Cathepsin B (CatB; EC 3.4.22.1), a cysteine lysosomal protease, has been suggested to promote the processing and secretion of mature-IL-1β by activated microglia (Halle et al., 2008; Terada et al., 2010; Sun et al., 2012; Wu et al., 2013). CatB also has beta secretase activity, which is involved in the processing of APP for Aβ formation (Hook et al., 2008, 2009).

We hypothesize that CatB is activated following systemic exposure to periodontal bacteria (or their components) and initiates the pathogenesis of AD. To test our hypothesis, we examined the effect of genetic CatB deficiency ($CatB^{-/-}$) and the administration of a specific CatB inhibitor on the learning and memory behavior, Aβ accumulation and microglia-mediated neuroinflammation using young adult and middle-aged mice after chronic systemic exposure to PgLPS.

2. Materials and methods

2.1. Animals

Heterozygous CatB (NM_007798.3)-deficient mice on a C57BL/6 background were maintained under specific-pathogen-free conditions at Kyushu University Faculty of Dental Sciences. Homozygous CatB-deficient ($CatB^{-/-}$) mice were generated by crossing heterozygous mice, and the lack of gene expression was confirmed by examining genomic DNA isolated from tail biopsies using a CatB-exon 4-specific polymerase chain reaction (PCR) with MCB11 primers (5′-GGTTGCGTTCGGTGAGG-3′) and MCBGT (5′-AACAAGAGC CGC AGG AGC-3′) (Sun et al., 2012; Terada et al., 2010; Wu et al., 2013).

Heterozygous mice were used as control animals in the present study and showed no pathological phenotypes when examined by histological, immunocytochemical or biochemical methods. All animals were treated in accordance with the protocols approved by the animal care and use committee of Kyushu University.

Wild-type adult mice (2 months old), middle-aged mice (12 months old) and age-matched $CatB^{-/-}$ mice (n = 6 in each group) were subjected to systemic exposure to PgLPS (1 mg/ml in deionized distilled water, DDW) daily (1 mg/kg/day, intraperitoneally; InvivoGen, CA, USA) for 5 weeks to mimic the chronic systemic inflammation induced by periodontits. Systemic exposure to DDW daily was performed in control mice as the negative control model.

2.2. Step-through passive avoidance test

The step-through avoidance test was performed in identical compartments consisting of illuminated and dark compartments with a grid floor and a guillotine door separating the compartments. In the acquisition trail, each mouse was placed in the light compartment and allowed to explore it for 30 s. The door of the dark compartment was then opened, and after the mouse stepped through the door, the door was closed and 2 electric shocks (0.6 mA, 16 s) were delivered through the grid. This training continued until the mouse stayed in the light compartment for 300 s. The retention trial was carried out every week until 5 weeks after training, and the latency was recorded for up to 300 s. The weight of the mouse was also evaluated every week until 5 weeks after training.

The non-stressed mice were allowed to step through the door without receiving an electric shock. Mice in each group were utilized in separated experiments (n = 6).

2.3. Locomotor activity

The spontaneous locomotor activity was measured in a clean, novel cage similar to the home cage, devoid of bedding or litter between 1:00 and 3:00 p.m. The cage was divide into four virtual quadrants, and the locomotor motor activity was measured by counting the number of line crossings and rearing incidents over a 5-min period.

2.4. Real-time quantitative PCR (RT-PCR) analysis

The mRNA was isolated from the MG6 microglia cell line after stimulation with PgLPS or pre-treatment with CA-074Me (Peptide Institute. Inc., Osaka, Japan), Bay (Sigma-Aldrich, St. Louis, MO, USA) or anti-TLR2 antibody (eBioscience, San Diego, CA, USA). The mRNA was also isolated from the hippocampal neurons after culture with microglial conditioned medium (MCM). Total mRNA was extracted with the RNAiso Plus (Takara, Hoto-ku, Osaka, Japan) in accordance with the manufacturer's instructions. A total of 800 ng of extracted mRNA was reverse transcribed to cDNA using the QuantiTect Reverse Transcription Kit (Qiagen, Hilden, Germany). After an initial denaturation step at 95 °C for 5 min, temperature cycling was initiated. Each cycle consisted of denaturation at 95 °C for 5 s, annealing at 60 °C for 10 s, and elongation for 30 s. In total, 40 cycles were performed. The cDNA was amplified in duplicate using a Rotor-Gene SYBR Green RT-PCR Kit (Qiagen) with a Corbett Rotor-Gene RG-3000A Real-Time PCR System. The data were evaluated using the RG-3000A software program (version Rotor-Gene 6.1.93, Corbett, Sydney, Australia). The sequences of primer pairs were as follows: CatB, 5′-GCAGC CAACTCTTGGAACCTT-3′ and 5′-GGATTCCAGCCACAATTTC TG-3′; IL-1β, 5′-CAACCAACAAGTGATATTCTCCATG-3′ and 5′-GATCCA CACTCTCCAGCTGCA-3′; APP, 5′-CGGAAGAGATCTCGGAAGTG-3′ and 5′-TGTTCGAACCCACATCTTCA-3′; TLR2, 5′-CCATCGAAAAGAGC CACA-3′ and 5′-CAGCAAAACAAGGATGGC-3′; BACE1, 5′-GATGGTG GACAACCTGAG-3′ and 5′-CTGGTAGTAGCGATGCAG-3′.

For data normalization, the mRNA expression of actin was measured, and the relative units were calculated by a comparative Ct method. All of the real-time RT-PCR experiments were repeated three times, and the results are presented as the means of the ratios ± standard error of the mean (SEM).

2.5. Immunoblotting analyses

The hippocampus was isolated from the young and middle-aged groups with and without PgLPS exposure. The tissues were quickly frozen and stored until use at −80 °C. The immunoblotting analysis was conducted as described previously (Sun et al., 2012). In brief, each tissue sample was homogenized and separated using 15%, 12% or 7.5% SDS-polyacrylamide gels. The proteins on the SDS gels were then transferred to nitrocellulose membranes. Following blocking the membranes were incubated at 4 °C overnight under gentle agitation with each primary antibody: goat anti-CatB (S-12; 1:1000; Santa Cruz, CA, USA), mouse anti-IL1β (Fxo2; 1:1000; Santa Cruz), mouse anti-TLR2 (T2.5; 1:500; eBioscience), TLR4 (1:500; eBioscience) rabbit anti-APP (ab15272; 1:3000; abcam, Cambridge, UK), rabbit anti-IκBα (SC-847; 1:1000; Santa Cruz) and mouse anti-actin (ab8226; 1:5000; abcam). After washing, the membranes were incubated with horseradish peroxidase anti-mouse (1:2000; R&D Systems, Minneapolis, USA) or anti-rabbit (1:2000; GE Healthcare, Buckinghamshire, UK) for 2 h at room temperature. Subsequently, the membrane-bound, HRP-labeled antibodies were detected using an enhanced chemiluminescence detection system (ECK lit; GE Healthcare) with an image analyzer (LAS-1000; Fuji Photo, Film Minato-ku Tokyo, Japan).

2.6. Immunofluorescent staining

The middle-aged wild-type and *CatB*$^{-/-}$ mice were anesthetized and killed by intracardiac perfusion with PBS. After perfusion, the brain was removed and further fixed by immersion in 4% paraformaldehyde overnight at 4 °C and then cryoprotected for 2 days in 30% sucrose in PBS and embedded in optimal cutting temperature compound (Sakura Finetechnical). Serial coronal frozen sections (14 μm thick) were prepared as previously reported (Wu et al., 2008). The sections were washed with PBS plus 0.1% TritonX-100 for 10 min at 24 °C and then incubated with the primary antibodies as follows: goat anti-CatB (1:1000; Santa Cruz), rabbit anti-Iba1 (1:10,000; Wako, Osaka, Japan), rabbit anti-GFAP (1:5000; Sigma-Aldrich, St. Louis, MO, USA) or NeuroTrace Fluorescent Nissl Stains (1:200; Molecular Probes Waltham, Massachusetts, USA), rat anti-lysosome-associated membrane protein 2 (GL2A7; LAMP2; 1:500 abcam), rabbit anti-Iba1 or mouse anti-$A\beta_{1-42}$ (1:500; QED BIOSCIENCE, San Diego, CA, USA); goat anti-cleaved IL-1β (m118, 1:100; Santa Cruz) and anti-TLR2 (1:500; eBioscience) at 4 °C overnight. After washing with PBS, the sections were incubated with donkey anti-goat Alexa 488 (1:500; Jackson ImmunoResearch, West Grove, PA, USA), donkey anti-rabbit Cy3 (1:500; Jackson ImmunoResearch), donkey anti-mouse Cy3 (1:500; Jackson ImmunoResearch), donkey anti-rabbit Cy3 (1:500; Jackson ImmunoResearch), donkey anti-goat Alexa 488 (1:500; Jackson ImmunoResearch) and donkey anti-mouse Alexa 488 (1:500; Jackson ImmunoResearch) at 4 °C for 2 h. The sections were then incubated with Hoechst (1:200; Sigma-Aldrich) and mounted in Vectashield anti-fading medium (Vector Laboratories, CA, USA). Fluorescence images were taken using a CLSM (C2si; Nikon, Japan).

The cultured hippocampal neurons were fixed with 4% paraformaldehyde for 48 h after incubation with MCM and incubated with rabbit anti-Aβ, mouse anti-microtubule-associated protein 2 (MAP2, 1:1000; Millipore, California, USA) or rat anti-LAMP2 overnight at 4 °C. After washing with PBS, the sections were incubated with donkey anti-rabbit Alexa 488, donkey anti-rabbit Cy3 or donkey anti-rat Cy3 at 4 °C for 2 h, and then incubated with Hoechst and mounted in Vectashield anti-fading medium. Fluorescence images were taken using a CLSM (C2si; Nikon).

2.7. ELISA assay for $A\beta_{1-42}$ and p65

The hippocampal neurons were cultured with MCM for 48 h and the level of Aβ measured using an enzyme-linked immunosorbent assay (ELISA) kit (MYBioSource, San Diego, CA, USA), NFκB-p65 was measured using an ELISA kit (IMGENEX, San Diego, CA USA) in accordance with the manufacturer's protocol. The absorbency at 450 nm was measured using a microplate reader.

2.8. Cell culture

The c-myc-immortalized mouse microglial cell line MG6 cells (Riken Cell Bank, Ibaraki, Japan) was maintained in DMEM containing 10% fetal bovine serum (Gibco, Grand Island, NY, USA) supplemented with 100 μM β-mercaptoethanol, 10 μg/ml insulin, 1% penicillin-streptomycin (Gibco) and 450 mg/ml glucose (Gibco) in accordance with the previously described methods (Sun et al., 2012; Wu et al., 2013). The primary microglia were isolated from the mixed primary cell culture obtained from the cerebral cortex of P1 wild-type and *CatB*$^{-/-}$ mice in accordance with the previously described methods (Ni et al., 2015). The cultured cells were stimulated with PgLPS (1 μg/ml; InvivoGen) or pre-treatment with CA-074Me (Peptide Institute Inc., Osaka, Japan), Bay (11-7082; Sigma-Aldrich) or TLR2 antibody (T2.5; 1:500; eBioscience). The conditioned medium was harvested 48 h after stimulation. Hippocampal neurons were isolated from P1 wild-type mice, the hippocampus dissected, digested by papain (Worthington, IN, USA) and filtered using a 50-μm sterile nylon filter. The cells were maintained in Minimum Essential Medium (MEM; Gibco) containing 10% horse serum, 450 mg/ml glucose, 1% penicillin-streptomycin and 100 mM sodium pyruvate (Gibco) at 37 °C under 10% CO_2. After one day, the medium was changed to EAGLE'S MEM (Nissui Pharmaceutical Co., LTD, Minato-ku, Tokyo, Japan) with 2% B27 supplement (Gibco), 450 mg/ml Glucose, 1% penicillin-streptomycin (Gibco) and 200 mM L-glutamine (Gibco) for 2 weeks.

2.9. Statistical analyses

The data are represented as the means ± SEM. The statistical analyses were performed by a one- or two-way ANOVA with a post hoc Tukey's test using the GraphPad Prism software package (GraphPad Software, California, USA). A value of $p < 0.05$ was considered to indicate statistical significance.

3. Results

3.1. Chronic systemic exposure to PgLPS induces CatB-dependent learning and memory deficits in middle-aged mice

The learning and memory function was examined using the step-through passive avoidance test. Compared with the non-stressed mice and those subjected to systemic exposure to DDW, mice subjected to systemic exposure to PgLPS for one week did not show reduced latency in young adult or middle-aged WT mice or in age-matched *CatB*$^{-/-}$ mice (Fig. 1A, B). Similarly, chronic exposure to PgLPS for five weeks also did not reduce the latency in young adult mice (Fig. 1A). However, systemic exposure to PgLPS for 5 weeks significantly reduced the latency in middle-aged WT mice, but not in middle-aged *CatB*$^{-/-}$ mice (Fig. 1B), indi-

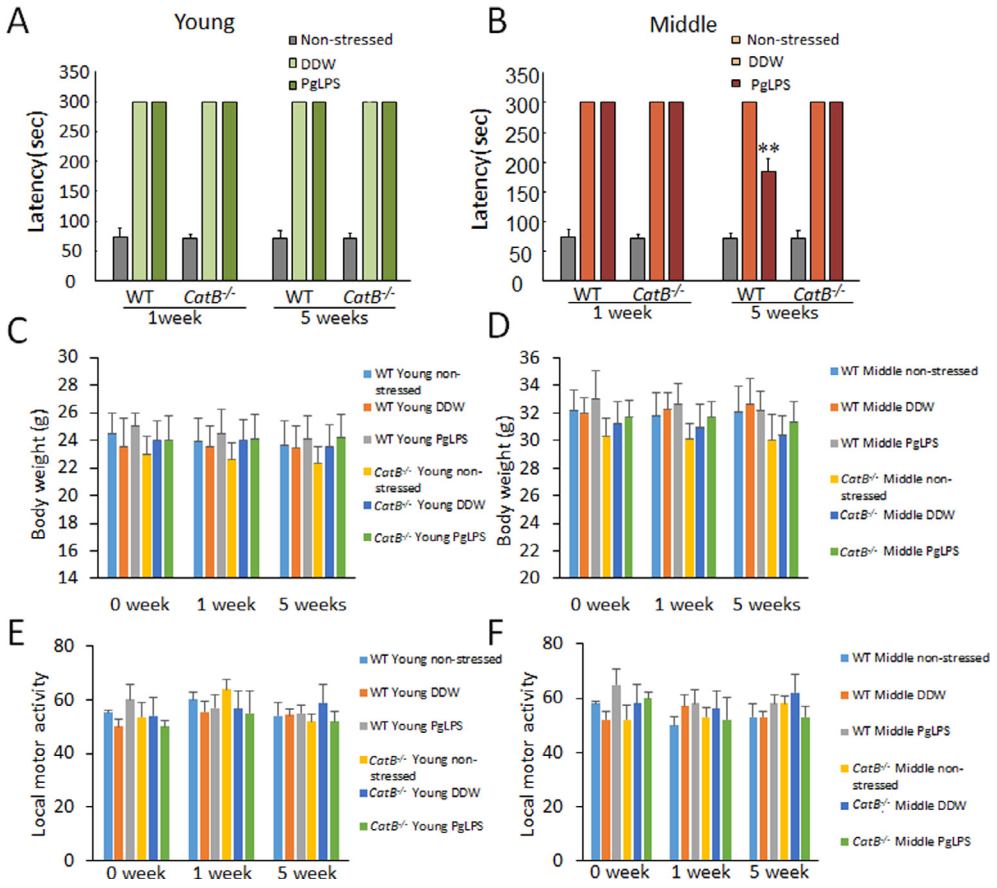

Fig. 1. Chronic systemic exposure to PgLPS induces CatB-dependent learning and memory deficits in middle-aged mice. (A) Exposure to PgLPS for five weeks did not induced learning or memory deficits in young adult mice. (B) Exposure to PgLPS for five weeks induced learning and memory deficits in middle-aged WT mice, which was significantly inhibited by CatB deficiency ($CatB^{-/-}$). (C) Exposure to PgLPS for five weeks did not change the body weight in young adult mice. (D) Exposure to PgLPS for five weeks did not change the body weight in middle-aged mice. (E) Exposure to PgLPS for five weeks did not change the local motor activity in young adult mice. (F) Exposure to PgLPS for five weeks did not change the local motor activity in middle aged mice. Each column and bar represents the means ± SEM (n = 6, each). Asterisks indicate a statistically significant difference from the value for exposure to DDW ($^{**}p < 0.01$, one-way ANOVA test).

cating that chronic systemic exposure to PgLPS is associated with learning and memory deficits only in middle age, which are prevented by CatB deficiency. Chronic systemic exposure to PgLPS did not reduce the body weight (Fig. 1C, D) or other sickness-related symptoms, such as local motor activity (Fig. 1E, F), in any of the PgLPS-exposed mice, suggesting that the PgLPS-induced learning and memory deficits in middle-aged mice are not associated with sickness behaviors. No mortality or other signs of morbidity were detected at the dose of PgLPS used in our study (1 mg/kg/d).

3.2. Chronic systemic exposure to PgLPS increases CatB production in both microglia and neuron in the middle-aged mice

Since CatB deficiency prevented the PgLPS-induced learning and memory deficits in mice, we next explored the CatB expression in the hippocampus of WT mice after chronic systemic exposure to PgLPS. Exposure to PgLPS significantly increased the expression of mature CatB in the hippocampus of middle-aged mice compared to middle-aged mice exposed to DDW (Fig. 2A, B). However, the expression of mature CatB wasn't detected in $CatB^{-/-}$ mice (Fig. 2A, B). Immunofluorescent images showed the cellular source of CatB to be the hippocampal CA1 subfield after systemic exposure to PgLPS. The expression of CatB was significantly increased in Iba1-positive microglia (6-fold increase) and Nissl-positive neurons (2-fold increase), but not in GFAP-positive astrocytes in the CA1 subfield of the hippocampus (Fig. 2C, D). These results indicate that chronic systemic exposure to PgLPS increased the expression of CatB in both microglia and neurons in the hippocampus of middle-aged mice.

3.3. Chronic systemic exposure to PgLPS increases CatB-dependent mIL-1β production in microglia in middle-aged mice

Next, the effects of systemic exposure to PgLPS on mature IL-1β production were examined, as CatB plays a key role in IL-1β proteolytic processing (Sun et al., 2012; Terada et al., 2010; Wu et al., 2013). The mIL-1β production was significantly increased in hippocampus of the middle-aged WT mice but not in the middle-aged $CatB^{-/-}$ mice or young adult WT and $CatB^{-/-}$ mice (Fig. 3A, B). Immunofluorescent images confirmed that mIL-1β was significantly increased in Iba1-positive microglia (8-fold increase) but not in Nissl-positive neurons or GFAP-positive astrocytes in the CA1 subfield of hippocampus (Fig. 3C, D). These results indicate that chronic systemic exposure to PgLPS increases the mIL-1β production in microglia of middle-aged mice and is CatB-dependent.

3.4. Chronic systemic exposure to PgLPS increases CatB-dependent TLR2 and TLR4 expression in microglia in the middle-aged mice

We next assessed the effects of systemic exposure to PgLPS on the expression of TLR2 and TLR4, which have been shown to bind to PgLPS (Liu et al., 2013). TLR2 and TLR4 expression was signifi-

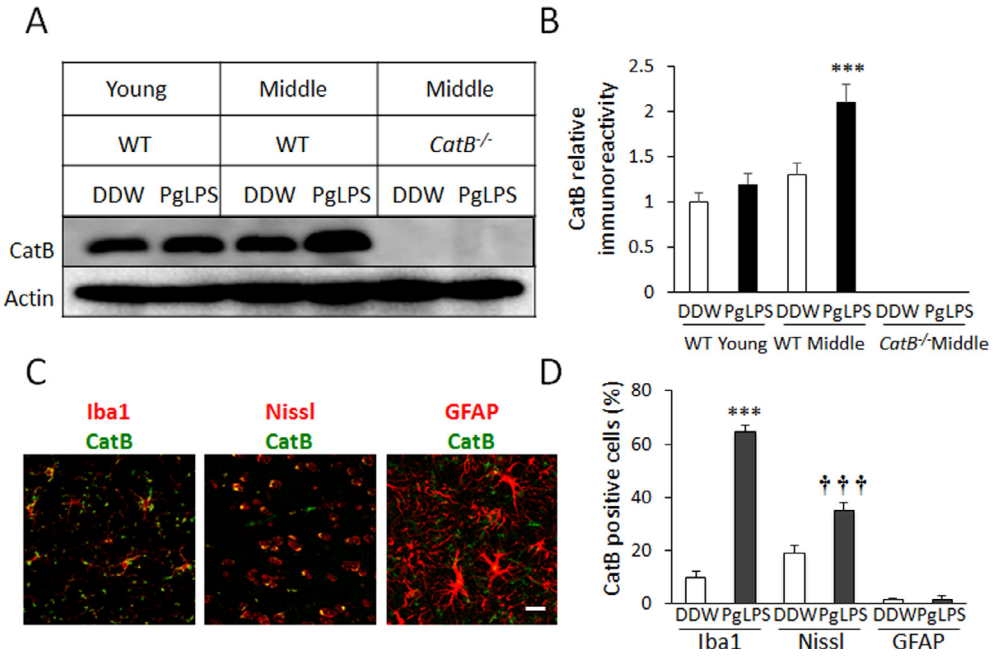

Fig. 2. Chronic systemic exposure to PgLPS increased CatB production in both microglia and neuron in the middle-aged mice. (A) Exposure to PgLPS for five weeks induced increases in mature CatB expression in the hippocampus of middle-aged mice, but not in that of young mice. No expression of mature CatB was detected in the $CatB^{-/-}$ mice. (B) The quantitative analyses of the immunoblot in (A). Each column and bar represents the means ± SEM (n = 6, each). Asterisks indicate a statistically significant difference from the value for young mice ($^{***}p < 0.001$, two-way ANOVA test). (C) Immunofluorescent CLMS images show the localization of CatB (green) in microglia (Iba1, red), neurons (Nissl, red) and astrocytes (GFAP, red) in the hippocampus CA1 region per section prepared from middle-aged mice after chronic systemic exposure to PgLPS. Scale bar, 25 μm. (D) The mean percentage of CatB-positive microglia (Iba1), neurons (Nissl) and astrocytes (GFAP) in (C). Each column and bar represents the means ± SEM (n = 6, each). Asterisks indicate a statistically significant difference from the value for DDW ($^{***}p < 0.01$, two-way ANOVA test). (For interpretation of the references to colour in this figure legend, the reader is referred to the web version of this article.)

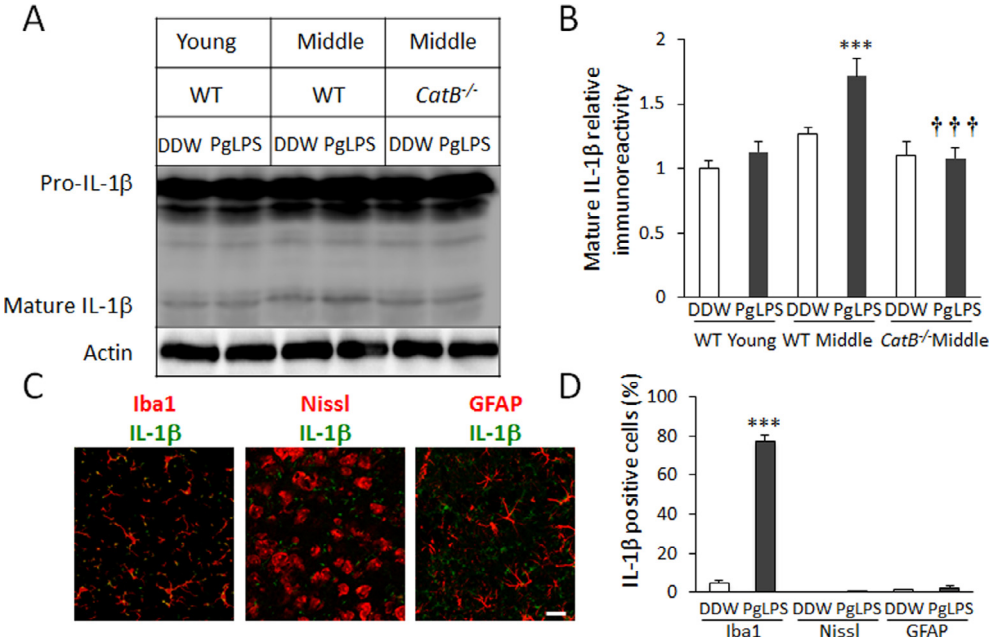

Fig. 3. Chronic systemic exposure to PgLPS induces CatB-dependent mIL-1β production in microglia in middle-aged mice. (A) Exposure to PgLPS for five weeks induces mIL-1β production in the brain of middle-aged WT mice, but not in that of young mice or middle-aged $CatB^{-/-}$ mice. (B) The quantitative analyses of the mIL-1β immunoblot in (A). Each column and bar represents the means ± SEM (n = 6, each). Asterisks indicate a statistically significant difference from the value for young or middle-aged $CatB^{-/-}$ mice ($^{***}p < 0.001$, two-way ANOVA). (C) Immunofluorescent CLMS images show the localization of mIL-1β (green) in microglia (Iba1, red), neurons (Nissl, red) and astrocytes (GFAP, red) in the hippocampus CA1 region per section prepared from middle-aged mice after chronic systemic exposure to PgLPS. Scale bar, 25 μm. (D) The mean percentage of mIL-1β-positive microglia (Iba1), neurons (Nissl) and astrocytes (GFAP) in (C). Each column and bar represents the means ± SEM (n = 6, each). Asterisks indicate a statistically significant difference from the value for DDW ($^{***}p < 0.01$, two-way ANOVA test). (For interpretation of the references to colour in this figure legend, the reader is referred to the web version of this article.)

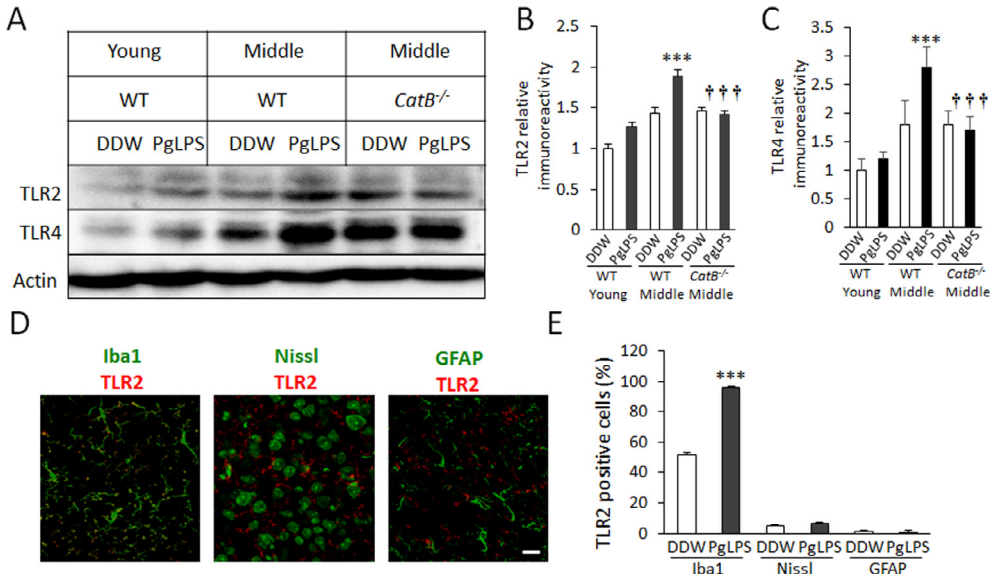

Fig. 4. Chronic systemic exposure to PgLPS induces CatB-dependent TLR2 expression in microglia in middle-aged mice. (A) Exposure to PgLPS for five weeks induces TLR2 expression in the brain of middle-aged mice, but not in that of young mice or middle-aged *CatB*$^{-/-}$ mice. (B, C) The quantitative analyses of the immunoblot of TLR2 (B) and TLR4 (C) in (A). Each column and bar represents the means ± SEM (n = 3, each). Asterisks indicate a statistically significant difference from the value for young or middle-aged *CatB*$^{-/-}$ mice ($^{***}p < 0.001$, two-way ANOVA test). (D) Immunofluorescent CLMS images show the localization of TLR2 (red) in microglia (Iba1, green), neurons (Nissl, green) and astrocytes (GFAP, green) in the hippocampus CA1 region per section prepared from middle-aged mice after chronic systemic exposure to PgLPS. Scale bar, 25 μm. (E) The mean percentage of TLR2-positive microglia (Iba1), neurons (Nissl) and astrocytes (GFAP) in (D). Each column and bar represents the means ± SEM (n = 6, each). Asterisks indicate a statistically significant difference from the value for DDW ($^{***}p < 0.01$, two-way ANOVA test). (For interpretation of the references to colour in this figure legend, the reader is referred to the web version of this article.)

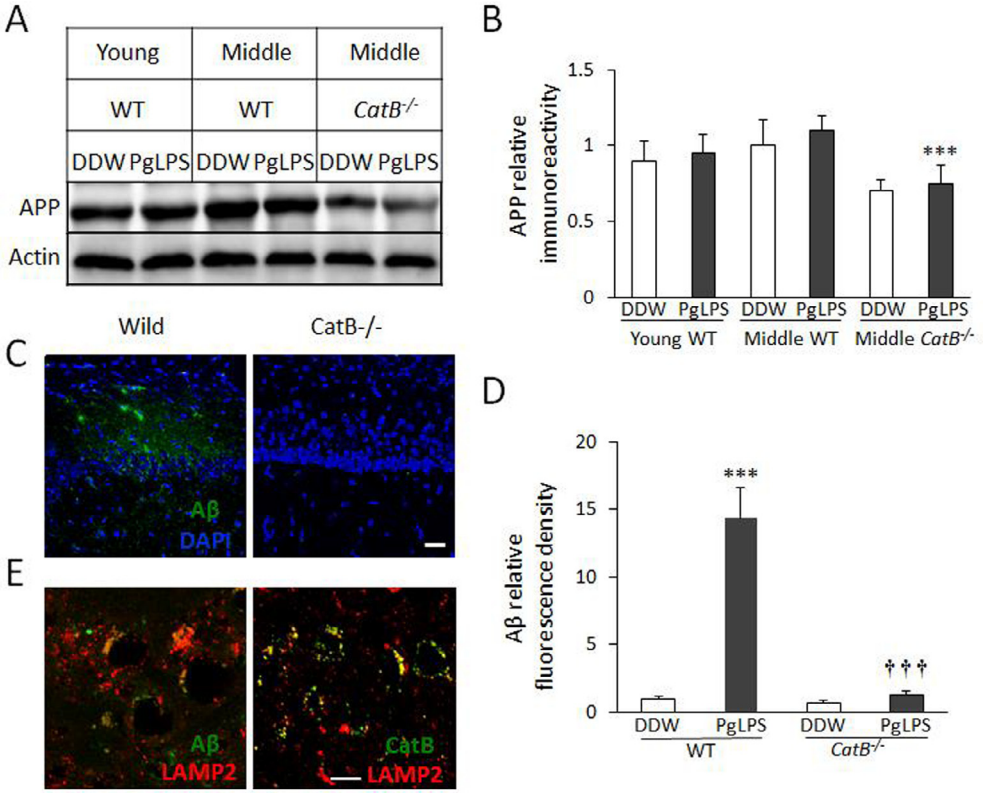

Fig. 5. Chronic systemic exposure to PgLPS induces CatB-dependent Aβ accumulation in neuron in middle-aged mice. (A) Exposure to PgLPS for five weeks induces APP production in the brain of middle-aged WT mice, but not in that of young mice or middle-aged *CatB*$^{-/-}$ mice. (B) The quantitative analyses of the APP immunoblot in (A). Each column and bar represents the means ± SEM (n = 6, each). Asterisks indicate a statistically significant difference from the value for middle-aged *CatB*$^{-/-}$ mice ($^{***}p < 0.001$, one-way ANOVA). (C) Immunofluorescent CLMS images show the Aβ accumulation (green) in the hippocampus CA1 region per section prepared from middle-aged WT mice after chronic systemic exposure to PgLPS. Scale bar, 50 μm. (D) The mean fluorescence density of Aβ (C). Each column and bar represents the means ± SEM (n = 6, each). Asterisks indicate a statistically significant difference from the value for DDW or middle-aged *CatB*$^{-/-}$ mice ($^{***}p < 0.01$, one-way ANOVA test). (E) Immunofluorescent CLMS images shows that both Aβ (green) and CatB (green) are localized in the lysosomes (LAMP-2, red). Scale bar, 15 μm. (For interpretation of the references to colour in this figure legend, the reader is referred to the web version of this article.)

cantly increased in the hippocampus of the middle-aged WT mice but not in middle-aged *CatB*$^{-/-}$ mice or young adult WT and *CatB*$^{-/-}$mice (Fig. 4A, B). Immunofluorescent images confirmed that TLR2 was increased in Iba1-positive microglia (2-fold increase), while Nissl-positive neurons and GFAP positive astrocytes failed to show expression of TLR2 after 5 weeks of systemic exposure to PgLPS (Fig. 4C, D). TLR4 was detected in Iba1-positive microglia, Nissl-positive neurons and GFAP-positive astrocytes after 5 weeks of systemic exposure to PgLPS (data not shown). These results indicate that chronic systemic exposure to PgLPS increases the CatB-dependent microglia TLR2 expression in middle-aged mice.

3.5. Chronic systemic exposure to PgLPS induces CatB-dependent Aβ accumulation in neurons in middle-aged mice

We next examined the effects of systemic exposure to PgLPS on Aβ accumulation in the hippocampus of mice. The expression of amyloid precursor protein (APP) did not markedly differ between WT middle-aged and young mice, and the APP expression was significantly lower at baseline in the middle-aged *CatB*$^{-/-}$ mice than in the middle-aged WT mice (Fig. 5A, B). Immunofluorescent images show that the Aβ expression was significantly increased in the CA1 regions of the hippocampus in the middle-aged WT mice but not in the middle-aged *CatB*$^{-/-}$mice after 5 weeks of systemic exposure to PgLPS (Fig. 5C, D). Aβ and CatB were co-localized in the LAMP-2-positive phagolysosomes in neurons of middle-aged mice (Fig. 5E). These results indicate that chronic exposure to PgLPS increases the CatB-dependent intracellular Aβ accumulation in middle-aged WT mice.

3.6. PgLPS induces CatB-dependent activation of cultured microglia

To clarify the biological mechanisms by which PgLPS promotes neuroinflammation, we next assessed the effects of PgLPS on microglia *in vitro*. As shown in Fig. 6A and B, the mean TLR2 mRNA expression of MG6 microglia (Fig. 6A) and primary microglia (Fig. 6B) were significantly increased at 24 h after treatment with PgLPS (1 μg/ml). The PgLPS-induced increase in the mean TLR2 mRNA expression was significantly decreased after pre-incubation with Bay 11-7082 (specific NF-κB inhibitor, 20 μM) or CA-074Me (specific CatB inhibitor, 50 μM). As shown in Fig. 6C and D, the mean IL-1β mRNA expression in the cultured MG6 microglia (Fig. 6C) and primary microglia (Fig. 6D) was significantly increased at 24 h after treatment with PgLPS (1 μg/ml) and significantly decreased at 24 h after pre-incubation with the neutralizing antibodies against TLR2 (10 μg/ml) (but not by anti-TLR4 as reported by Liu et al., 2013), Bay 11-7082 (20 μM) or CA-074Me (50 μM). Nuclear translocation of p65 was significantly increased at 2 h after PgLPS treatment (Fig. 6E), which was suppressed by pre-incubation with neutralizing antibodies against TLR2 (Fig. 6E). Pre-incubation with CA-074Me had no effect on the early acute activation of NF-κB at 2 h after PgLPS treatment (Fig. 6E). Chronic activation of NF-κB was further examined by immunoblotting of IκBα after treatment with PgLPS. The mean protein level of IκBα was significantly decreased in a time-dependent manner after treatment with PgLPS (Fig. 6F, G). Taken together, these findings indicate that inhibition of CatB suppressed the PgLPS-enhanced expression of TLR2, IL-1β and NF-κB. These results demonstrate that PgLPS directly induces microglia activation in a CatB-dependent manner.

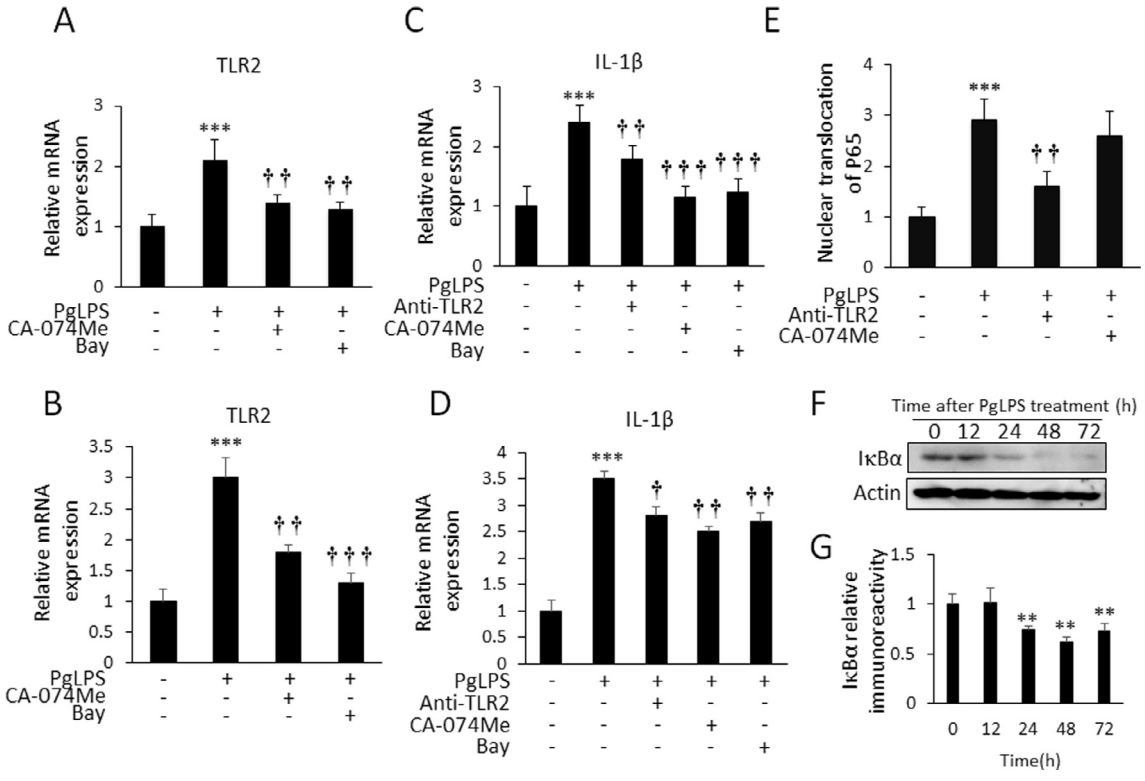

Fig. 6. PgLPS induces CatB-dependent activation of the cultured microglia. (A, B) The mean mRNA of TLR2 of MG6 microglia (A) and primary microglia (B) at 24 h after treatment with PgLPS. CA-074 Me (50 μM) or Bay 11-7082 (Bay, 20 μM) was used for pre-treatment for 1 h. (C, D) The mean mRNA of IL-1β of MG6 microglia (C) and primary microglia (D) at 24 h after incubation with PgLPS or pre-treatment with neutralizing antibodies against TLR2 (10 μg/ml), CA-074 Me (50 μM) or Bay 11-7082 (Bay, 20 μM). (E) The relative nuclear translocation of p65 1 h after treatment with PgLPS. Neutralizing antibodies against TLR2 (10 μg/ml) and CA-074 Me (50 μM) were used for pre-treatment for 1 h. (F) The time course of IκBα protein expression in MG6 microglia after treatment with PgLPS. (G) The quantitative analyses of total IκBα in the immunoblot shown in (F). Each column and bar represents mean ± SEM (n = 3), $^{***}P < 0.001$ versus non-treated cells (none). $^{\dagger\dagger\dagger}P < 0.001$ versus PgLPS alone (two-way ANOVA test).

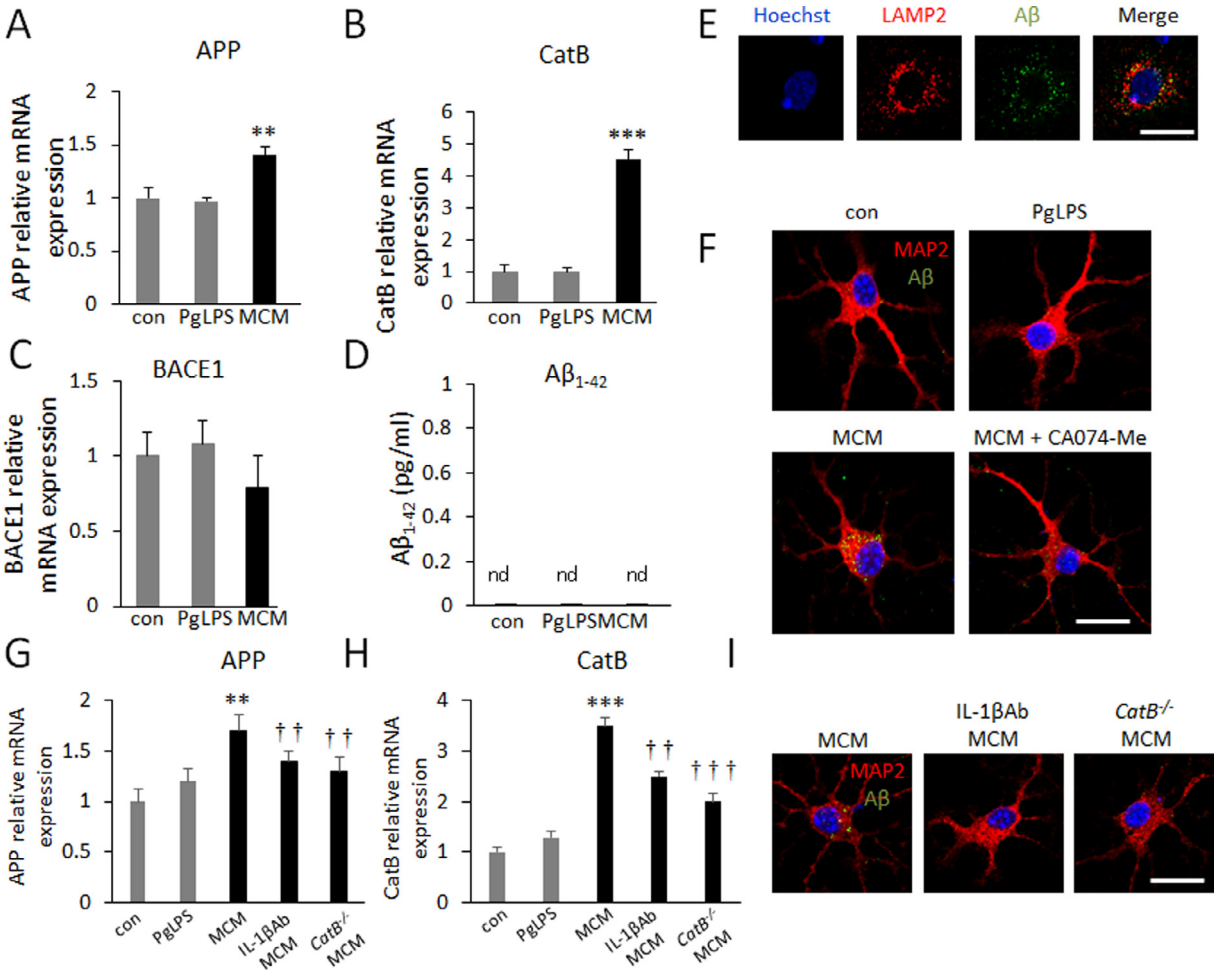

Fig. 7. PgLPS-induced CatB-dependent microglia activation is required for intracellular Aβ accumulation in the cultured primary hippocampal neurons. (A–C) The mean mRNA levels of APP (A), CatB (B) and BACE1 (C) in the cultured primary hippocampus neurons 24 h after treatment with PgLPS and the PgLPS-treated conditioned medium of microglia (MCM). (D) The secretion of Aβ from the hippocampal neurons after treatment with PgLPS and MCM (ELISA). Each column and bar represents the mean ± SEM ($n = 3$), $^{**}P < 0.01$, $^{***}P < 0.001$ versus non-treated cells (con). (E) Immunofluorescent CLMS images of MAP2 (red) and Aβ (green) in cultured primary hippocampus neurons with Hoechst-stained nuclei (blue) 48 h after treatment with PgLPS and MCM with or without 1 h pre-incubation with CA-074 Me. Scale bar, 25 μm. (F) Immunofluorescent CLMS images of LAMP2 (red) and Aβ (green) in cultured primary hippocampus neurons with Hoechst-stained nuclei (blue) 48 h after treatment with the conditioned medium of microglia. Scale bar, 25 μm. (G, H) The mean mRNA expression of APP (G) and CatB (H) in the cultured primary hippocampal neurons 24 h after treatment with PgLPS and the PgLPS-treated conditioned medium of primary WT and *CatB*$^{-/-}$ microglia pre-incubated with or without IL-1β neutralization antibody. Each column and bar represents the mean ± SEM ($n = 3$), $^{**}P < 0.01$, $^{***}P < 0.001$ versus non-treated cells (none). $^{\dagger\dagger\dagger}P < 0.001$ versus MCM group alone (two-way ANOVA test). (I) Immunofluorescent CLMS images of LAMP2 (red) and Aβ (green) in cultured primary hippocampus neurons with Hoechst-stained nuclei (blue) 48 h after treatment with the conditioned medium of primary microglia. Scale bar, 30 μm. (For interpretation of the references to colour in this figure legend, the reader is referred to the web version of this article.)

3.7. PgLPS induces the CatB-dependent microglia activation required for intracellular Aβ accumulation in primary cultured hippocampal neurons

To clarify whether the effects of PgLPS on the Aβ accumulation in neurons are exerted directly or indirectly via microglial activation, we treated cultured primary cultured hippocampal neurons with PgLPS or with microglial conditioned medium at 48 h after treatment with PgLPS. The mean APP mRNA expression of the cultured primary cultured hippocampal neurons was not changed 24 h after treatment with PgLPS (1 μg/ml). Surprisingly, a significantly increased mean APP mRNA was observed following incubation with PgLPS-treated conditioned medium of microglia (MCM) (Fig. 7A). Next, the mRNA expression of CatB and BACE1 was examined, as both have beta secretase activity and thus can cleave APP into $A\beta_{1-42}$ (Hook et al., 2008, 2010). The mean mRNA expression of CatB in the cultured primary hippocampus neurons was significantly increased at 24 h after incubation with MCM, while the expression of BACE1 was not markedly changed (Fig. 7C). The secretion of $A\beta_{1-42}$ was examined by ELISA, and neither MCM nor PgLPS induced secretion of $A\beta_{1-42}$ (Fig. 7D). Immunofluorescent CLMS images showed that Aβ was accumulated in LAMP-2-positive phagolysosomes incubated with MCM (Fig. 7E) but was not observed after direct PgLPS stimulation (Fig. 7F). The MCM-induced increase in Aβ accumulation was prevented by pre-incubation with CA-074Me (Fig. 7F).

To further confirm that the effects of microglia on neuronal APP and CatB expression were CatB- and IL-1β-dependent, MCM was collected from the primary WT and *CatB*$^{-/-}$ microglia treated with PgLPS or pre-treated with IL-1β neutralization antibody before treatment with PgLPS. This MCM was then used for the incubation of primary cultured hippocampal neurons. The mRNA expression of CatB and APP in the hippocampal neurons was significantly increased following incubation with PgLPS-treated MCM (Fig. 7G, H). However, the expression of the hippocampal APP and CatB were significantly decreased following incubation with PgLPS and IL-1β neutralization antibody-treated MCM and PgLPS-treated conditioned medium from *CatB*$^{-/-}$ microglia (Fig. 7G, H). Immunofluorescent CLMS images showed that Aβ was also accumulated in hippocampal neurons that had been incubated with primary

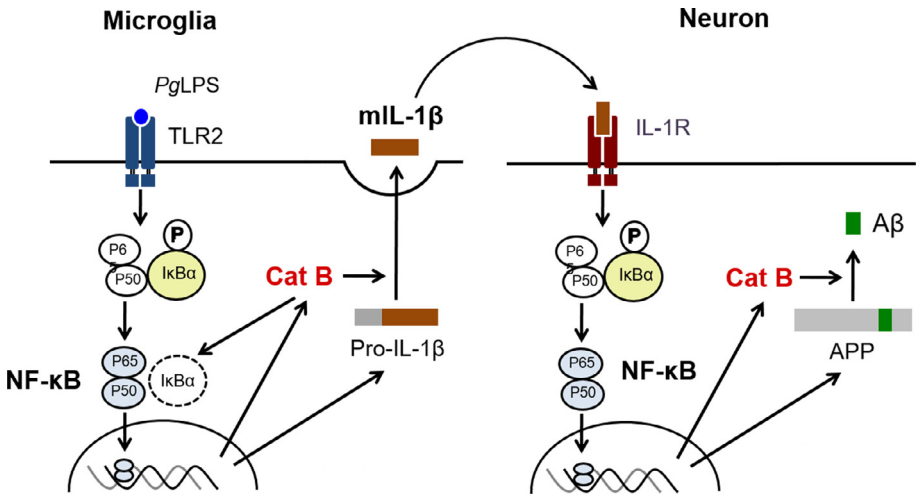

Fig. 8. A schematic representation of the critical roles of CatB in initiating AD-like phenotypes during chronic systemic PgLPS exposure. In microglia, PgLPS-induced CatB is involved in mIL-1β production and IκBα degradation for the chronically activation of TLR2/NFκB signaling, thus autocratically amplifying the microglia-mediated neuroinflammation. In contrast, the effects of PgLPS on neurons are microglia-dependent. The mIL-1β, the production of which is mediated by microglia, increases IL-1/NFκB-dependent CatB and APP production through IL-1R signaling. The increased CatB in neurons is involved in APP processing for Aβ accumulation directly and NF-κB activation for autocratic APP and CatB production.

MCM (Fig. 7I). The MCM-increased Aβ accumulation was prevented by pre-incubation with IL-1β neutralization antibody or MCM from *CatB*$^{-/-}$ microglia (Fig. 7I). These findings suggest that the CatB-dependent microglia activation induced by chronic exposure to PgLPS required for intracellular Aβ accumulation in neurons is CatB-dependent. The critical roles of CatB in the initiation of AD-like phenotypes following chronic systemic exposure to PgLPS are summarized in Fig. 8.

4. Discussion

The present study shows that chronic systemic exposure to PgLPS initiates AD-like phenotypes, including learning and memory deficits, intracellular Aβ accumulation in neurons and microglia-mediated neuroinflammation in the hippocampus of middle-aged mice. This is the first evidence supporting a causal association between chronic exposure to the components of periodontal bacteria and an AD-like phenotype in middle-aged mice. The critical roles of CatB in the effects mediated by PgLPS provide a novel mechanism for the correlation of chronic periodontitis with the onset and/or progression of AD.

Systemic exposure to PgLPS in mice for five consecutive weeks mimics chronic systemic exposure to bacterial components associated with periodontists in human for approximately 3.8 years, as the average lifespan of C57BL/6N mice is 1/40 of that of humans (Oeppen and Vaupel, 2002; Pyo et al., 2013). Sustained exposure to PgLPS induced a memory deficit in middle-aged mice but not in young adult mice, which is consistent with previous findings of memory deficit induction in middle-aged rats with chronic arthritis (Liu et al., 2012). Nerveless, periodontitis, as the most common avenue of chronic oral multi-bacterial exposure, induces and amplifies low-grade systemic inflammation, resulting in the relevant bacteria and their components entering the body through the systemic circulation (Pischon et al., 2007). Periodontitis is often contracted in middle-aged individuals (Albandar and Rams, 2002) and is associated with an exacerbation in the cognitive decline in AD patients (Kamer et al., 2008; Noble et al., 2009; Martande et al., 2014; Ide et al., 2016).

In the current study, we used the passive avoidance task to examine learning and memory behavior, as the hippocampus plays a key role in the passive avoidance learning and memory (Cahill and McGaugh, 1998; Campbell and Macqueen, 2004; Nyberg, 2005), which is particularly associated with memory deficits in AD (Antonenko et al., 2016; Douet et al., 2014; Metzler-Baddeley et al., 2012). Furthermore, the passive avoidance task is used to examine the effects of systemic infection on the memory function in mice (Dehkordi et al., 2015; Wang et al., 2013). Sustained systemic exposure to PgLPS did not reduce the body weight (Fig. 1C, D) or induce lethargy (Fig. 1E, F) during the experimental period, suggesting that the PgLPS-induced learning and memory deficits observed are not associated with sickness behaviors. These results conflict with previous findings that systemic exposure to *E. coli* LPS induces sickness behavior (Kahn et al., 2012; Kranjac et al., 2013; Sparkman et al., 2005). Our observations with PgLPS are similar to those noted with TLR2 agonists (Pam_3CSK_4 or lipoteichoic acid), which have less potency in mammals than TLR4 agonists such as *E. coli* LPS (Du et al., 2011; Eklind et al., 2004). The PgLPS-induced memory deficit in WT middle-aged mice was prevented in age-matched *CatB*$^{-/-}$ mice, and PgLPS exposure induced significant increases in CatB in both the microglia and neurons, suggesting that the memory deficit following systemic exposure to PgLPS in middle-aged mice is CatB-dependent.

PgLPS has been detected in the brain of AD patients (Poole et al., 2013), as well as fungal structures (Pisa et al., 2015). This has prompted a new hypothesis that, "Alzheimer's disease is caused by microbe infection" (Itzhaki et al., 2016). Generally, systemic administration of LPS does not access the brain directly due to the barrier functions of the BCSFB as well as the blood-brain barrier (BBB). We previously found that the permeability of BCSFB was increased in the middle-aged rats due to reduction of the tight junction proteins (occludin and ZO-1) during chronic systemic inflammation (Wu et al., 2008). This highly sensitive permeability of the BCSFB allows PgLPS to enter the brain, even in middle-aged animals. On the other hand, a recent study reported that the permeability of the BBB in middle-aged mice increased in an experimental model of autoimmune encephalomyelitis (Seo et al., 2015) and we have found that long-lasting alterations to cerebral vasculature has been in response to the systemic bacterial infection (Puntener et al., 2012). Further studies are needed to address whether the increased permeability of the BBB also contributes to the penetration of PgLPS in the middle-aged brain.

The purified PgLPS used in the present study has been show to bind both TLR2 and TLR4 (InvivoGen). However, we previously determined that TLR2 has high affinity binding to PgLPS in micro-

glia (Liu et al., 2013). The TLR2 expression significantly increased in the microglia of PgLPS-infected middle aged mice and the TLR2 expression was significantly reduced by in genetic and pharmacological inhibition of CatB. TLR2 transcription is tightly regulated by NF-κB activation, as its promoter contains NF-κB binding sites (Wang et al., 2001). There are at least two possibilities for CatB-mediated in TLR2 expression. One possibility is that CatB may be involved in the proteolytic degradation of IκBα and subsequent nuclear translocation of NF-κB (Ni et al., 2015; Fig. 6). The other possibility is that CatB may be involved in the distribution of TLR2 in phagolysosomes, as exposure to PgLPS increased the CatB expression in phagolysosomes (Fig. 5) and localization of TLR2 in phagolysosomes depends on NF-κB activation (Brandt et al., 2013; Fukui et al., 2001). Further studies are necessary to address the second possibility.

PgLPS-induced production of IL-1β in microglia was significantly suppressed by genetic and pharmacological inhibition of CatB, indicating that CatB plays a critical role in PgLPS-induced neuroinflammation. Furthermore, CA-074Me significantly inhibited the degradation of IκBα from 24 to 72 h, but not the translocation of p65 to the nucleus at 2 h in PgLPS-treated microglia, suggesting that CatB may prevent the transition of IL-β and subsequent neuroinflammation via inhibiting chronic activation of NFκB (Ni et al., 2015). Taken together, these findings suggest that CatB is involved in the activation of TLR2/NF-κB signaling during chronic systemic exposure to PgLPS.

$A\beta_{1-42}$ and CatB accumulated in the hippocampal neurons of PgLPS-exposed middle-aged WT mice, but not in those of PgLPS-exposed middle-aged $CatB^{-/-}$ mice (Figs. 2, 5). These observations suggest that CatB is involved in the PgLPS-induced accumulation of $A\beta_{1-42}$ in neurons. This is the first evidence that systemic exposure to a competent of periodontal bacteria (TLR2 agonist) increased the intracellular accumulation of Aβ in neurons, which had previously only been shown by TLR4 agonist in APPsweTg mice (Sheng et al., 2003) and WT mice (Kahn et al., 2012; Lee et al., 2008). The accumulation of $A\beta_{1-42}$ in the neurons of middle-aged mice is important for initiating AD-like phenotypes in the brain, as the intracellular accumulation of Aβ, particularly $A\beta_{1-42}$, which precedes amyloid deposits in AD (Cataldo et al., 2004; Gouras et al., 2000; Sheng et al., 2003), and the chronic burden of intracellular Aβ is toxic to degenerated neurons (Billings et al., 2005; Sheng et al., 2003). PgLPS may be involved in the chronic deposition of Aβ in degenerated neurons, as PgLPS has been detected in the brains of AD patients (Poole et al., 2013).

PgLPS-induced Aβ was co-localized with CatB in the LAMP-2 positive phagolysosomes in neurons of middle-aged mice (Figs. 5, 7), implying that CatB mediates the PgLPS-induced Aβ accumulation in phagolysosomes. Such endosomal/lysosomal Aβ production is important for the onset and progression of AD, as the increased expression and activation of CatB in lysosomes are the earliest neuropathological signs of AD before the onset of dementia (Pasternak et al., 2004), which precedes extracellular Aβ deposition and plaque formation in AD (D'Andrea et al., 2001; Gouras et al., 2000; Gyure et al., 2001; Pasternak et al., 2004). PgLPS induced Aβ accumulation in middle aged WT mice but not in the young adult mice, and the protein levels of APP in the PgLPS-exposed middle-aged $CatB^{-/-}$ mice were significantly lower than in the middle aged WT mice, suggesting that the PgLPS-induced CatB-mediated Aβ accumulation was age-dependent. These observations agreed with a previous finding of Aβ accumulation in autophagy-endosomal-lysosomal vesicles in aged mice (Yu et al., 2005). The age-related Aβ accumulation in endosomes/lysosomes may be related to an altered intracellular APP metabolism (Nakanishi et al., 1997), as approximately 30% of the total cellular APP resides in the lysosome (Pasternak et al., 2004). Aβ amyloidogenesis is favored in phagolysosomes acidification (Inouye and Kirschner, 2000; Knops et al., 1995; Schrader-Fischer and Paganetti, 1996), and the acidic microenvironment of endosomes/lysosomes is favorable for the toxic aggregation of Aβ in mammalian neurons (Su and Chang, 2001).

Chronic systemic exposure to PgLPS may alter the proteolytic environment for CatB-dependent Aβ accumulation in phagolysosomes. The microglia-mediated neuroinflammation is responsible for the PgLPS-induced CatB-mediated Aβ accumulation in neurons. First, MCM (conditioned medium from PgLPS-treated microglia from WT mice) but not PgLPS itself significantly increased the expression of APP in the cultured primary cultured hippocampal neurons (Fig. 7), which was increased following inflammation as an acute reaction protein (Sheng et al., 2003). Second, MCM of WT microglia significantly increased the expression of CatB in cultured primary hippocampal neurons, which was significantly inhibited by MCM of $CatB^{-/-}$ microglia. Third, PgLPS induced CatB/NF-κB-dependent IL-1β expression, which regulates the expression and processing of APP (Buxbaum et al., 1992; Rogers et al., 1999; Sheng et al., 2003). Fourth, the expression of APP and CatB in the primary cultured hippocampal neurons significantly decreased by MCM pre-treated with IL-1β neutralization antibody from the WT mice in comparison to the non-treated one. These observations further confirm the specific role of microglia in the expression of APP and CatB in neurons, as we previously reported a critical role of CatB in IL-1β production (Terada et al., 2010, Sun et al., 2012; Wu et al., 2013). Intriguingly, MCM did not affect the expression of aspartyl protease BACE1 expression, a β-secretase of APP (Vassar et al., 1999), which was further evidenced by the lack of any release of Aβ from MCM-treated primary cultured hippocampal neurons (Fig. 7). These findings indicate that PgLPS-increased CatB expression by microglia plays a critical role in the intracellular Aβ accumulation in neurons.

In conclusion, chronic systemic exposure to PgLPS, a component of periodontal bacteria, induces AD-like phenotypes, including learning and memory deficits, microglia-mediated neuroinflammation and Aβ accumulation, in middle-aged mice; in addition, these effects are CatB-dependent (Fig. 8). These observations strongly suggest that CatB plays a critical role in the link between periodontitis and AD. Therefore, CatB may be a therapeutic target for preventing periodontitis-associated cognitive decline in AD.

Conflict of interests

The authors declare that they have no conflict of interests in association with this study.

Acknowledgments

This work was supported by Grants-in-Aid for Scientific Research – Japan to Zhou Wu (16K11478) and Daiwa Anglo-Japanese Foundation (2015) to Jessica L. Teeling and Zhou Wu.

Appendix A. Supplementary data

Supplementary data associated with this article can be found, in the online version, at http://dx.doi.org/10.1016/j.bbi.2017.06.002.

References

Albandar, J.M., Rams, T.E., 2002. Risk factors for periodontitis in children and young persons. Periodontology 2000 (29), 207–222.
Antonenko, D., Kulzow, N., Cesarz, M.E., Schindler, K., Grittner, U., Floel, A., 2016. Hippocampal pathway plasticity is associated with the ability to form novel memories in older adults. Front. Aging Neurosci. 8, 61.

Billings, L.M., Oddo, S., Green, K.N., McGaugh, J.L., LaFerla, F.M., 2005. Intraneuronal Abeta causes the onset of early Alzheimer's disease-related cognitive deficits in transgenic mice. Neuron 45, 675–688.
Blennow, K., de Leon, M.J., Zetterberg, H., 2006. Alzheimer's disease. Lancet 368, 387–403.
Brandt, K.J., Fickentscher, C., Kruithof, E.K., de Moerloose, P., 2013. TLR2 ligands induce NF-kappaB activation from endosomal compartments of human monocytes. PLoS One 8, e80743.
Buxbaum, J.D., Oishi, M., Chen, H.I., Pinkas-Kramarski, R., Jaffe, E.A., Gandy, S.E., Greengard, P., 1992. Cholinergic agonists and interleukin 1 regulate processing and secretion of the Alzheimer beta/A4 amyloid protein precursor. Proc. Natl. Acad. Sci. U.S.A. 89, 10075–10078.
Cahill, L., McGaugh, J.L., 1998. Mechanisms of emotional arousal and lasting declarative memory. Trends Neurosci. 21, 294–299.
Campbell, S., Macqueen, G., 2004. The role of the hippocampus in the pathophysiology of major depression. J. Psychiatry Neurosci. 29, 417–426.
Cataldo, A.M., Peterhoff, C.M., Schmidt, S.D., Terio, N.B., Duff, K., Beard, M., Mathews, P.M., Nixon, R.A., 2004. Presenilin mutations in familial Alzheimer disease and transgenic mouse models accelerate neuronal lysosomal pathology. J. Neuropathol. Exp. Neurol. 63, 821–830.
D'Andrea, M.R., Nagele, R.G., Wang, H.Y., Peterson, P.A., Lee, D.H., 2001. Evidence that neurones accumulating amyloid can undergo lysis to form amyloid plaques in Alzheimer's disease. Histopathology 38, 120–134.
Dehkordi, N.G., Noorbakhshnia, M., Ghaedi, K., Esmaeili, A., Dabaghi, M., 2015. Omega-3 fatty acids prevent LPS-induced passive avoidance learning and memory and CaMKII-alpha gene expression impairments in hippocampus of rat. Pharmacol. Rep. 67, 370–375.
Douet, V., Chang, L., Cloak, C., Ernst, T., 2014. Genetic influences on brain developmental trajectories on neuroimaging studies: from infancy to young adulthood. Brain Imaging Behav 8, 234–250.
Du, X., Fleiss, B., Li, H., D'Angelo, B., Sun, Y., Zhu, C., Hagberg, H., Levy, O., Mallard, C., Wang, X., 2011. Systemic stimulation of TLR2 impairs neonatal mouse brain development. PLoS One 6, e19583.
Edison, P., Archer, H.A., Gerhard, A., Hinz, R., Pavese, N., Turkheimer, F.E., Hammers, A., Tai, Y.F., Fox, N., Kennedy, A., Rossor, M., Brooks, D.J., 2008. Microglia, amyloid, and cognition in Alzheimer's disease: an [11C](R)PK11195-PET and [11C]PIB-PET study. Neurobiol. Dis. 32, 412–419.
Eklind, S., Arvidsson, P., Hagberg, H., Mallard, C., 2004. The role of glucose in brain injury following the combination of lipopolysaccharide or lipoteichoic acid and hypoxia-ischemia in neonatal rats. Dev. Neurosci. 26, 61–67.
Fukui, A., Inoue, N., Matsumoto, M., Nomura, M., Yamada, K., Matsuda, Y., Toyoshima, K., Seya, T., 2001. Molecular cloning and functional characterization of chicken toll-like receptors. A single chicken toll covers multiple molecular patterns. J. Biol. Chem. 276, 47143–47149.
Gouras, G.K., Tsai, J., Naslund, J., Vincent, B., Edgar, M., Checler, F., Greenfield, J.P., Haroutunian, V., Buxbaum, J.D., Xu, H., Greengard, P., Relkin, N.R., 2000. Intraneuronal Abeta42 accumulation in human brain. Am. J. Pathol. 156, 15–20.
Gyure, K.A., Durham, R., Stewart, W.F., Smialek, J.E., Troncoso, J.C., 2001. Intraneuronal abeta-amyloid precedes development of amyloid plaques in Down syndrome. Arch. Pathol. Lab. Med. 125, 489–492.
Halle, A., Hornung, V., Petzold, G.C., Stewart, C.R., Monks, B.G., Reinheckel, T., Fitzgerald, K.A., Latz, E., Moore, K.J., Golenbock, D.T., 2008. The NALP3 inflammasome is involved in the innate immune response to amyloid-beta. Nat. Immunol. 9, 857–865.
Hickman, S.E., Allison, E.K., El Khoury, J., 2008. Microglial dysfunction and defective beta-amyloid clearance pathways in aging Alzheimer's disease mice. J. Neurosci. 28, 8354–8360.
Hook, V.Y., Kindy, M., Hook, G., 2008. Inhibitors of cathepsin B improve memory and reduce beta-amyloid in transgenic Alzheimer disease mice expressing the wild-type, but not the Swedish mutant, beta-secretase site of the amyloid precursor protein. J. Biol. Chem. 283, 7745–7753.
Hook, V.Y., Kindy, M., Reinheckel, T., Peters, C., Hook, G., 2009. Genetic cathepsin B deficiency reduces beta-amyloid in transgenic mice expressing human wild-type amyloid precursor protein. Biochem. Biophys. Res. Commun. 386, 284–288.
Hook, V., Hook, G., Kindy, M., 2010. Pharmacogenetic features of cathepsin B inhibitors that improve memory deficit and reduce beta-amyloid related to Alzheimer's disease. Biol. Chem. 391, 861–872.
Ide, M., Harris, M., Stevens, A., Sussams, R., Hopkins, V., Culliford, D., Fuller, J., Ibbett, P., Raybould, R., Thomas, R., Puenter, U., Teeling, J., Perry, V.H., Holmes, C., 2016. Periodontitis and cognitive decline in Alzheimer's disease. PLoS One 11, e0151081.
Inouye, H., Kirschner, D.A., 2000. A beta fibrillogenesis: kinetic parameters for fibril formation from congo red binding. J. Struct. Biol. 130, 123–129.
Itzhaki, R.F., Lathe, R., Balin, B.J., Ball, M.J., Bearer, E.L., et al., 2016. Microbes and Alzheimer's disease. J. Alzheimers Dis. 51 (4), 979–984.
Kahn, M.S., Kranjac, D., Alonzo, C.A., Haase, J.H., Cedillos, R.O., McLinden, K.A., Boehm, G.W., Chumley, M.J., 2012. Prolonged elevation in hippocampal Abeta and cognitive deficits following repeated endotoxin exposure in the mouse. Behav. Brain Res. 229, 176–184.
Kamer, A.R., Craig, R.G., Dasanayake, A.P., Brys, M., Glodzik-Sobanska, L., de Leon, M. J., 2008. Inflammation and Alzheimer's disease: possible role of periodontal diseases. Alzheimer's & dementia: the journal of the Alzheimer's Association 4, 242–250.
Knops, J., Suomensaari, S., Lee, M., McConlogue, L., Seubert, P., Sinha, S., 1995. Cell-type and amyloid precursor protein-type specific inhibition of A beta release by bafilomycin A1, a selective inhibitor of vacuolar ATPases. J. Biol. Chem. 270, 2419–2422.
Kranjac, D., Koster, K.M., Kahn, M.S., Eimerbrink, M.J., Womble, B.M., Cooper, B.G., Chumley, M.J., Boehm, G.W., 2013. Peripheral administration of D-cycloserine rescues memory consolidation following bacterial endotoxin exposure. Behav. Brain Res. 243, 38–43.
Lee, J.W., Lee, Y.K., Yuk, D.Y., Choi, D.Y., Ban, S.B., Oh, K.W., Hong, J.T., 2008. Neuro-inflammation induced by lipopolysaccharide causes cognitive impairment through enhancement of beta-amyloid generation. J. Neuroinflammation 5, 37.
Liu, X., Wu, Z., Hayashi, Y., Nakanishi, H., 2012. Age-dependent neuroinflammatory responses and deficits in long-term potentiation in the hippocampus during systemic inflammation. Neuroscience 216, 133–142.
Liu, Y., Wu, Z., Zhang, X., Ni, J., Yu, W., Zhou, Y., Nakanishi, H., 2013. Leptomeningeal cells transduce peripheral macrophages inflammatory signal to microglia in response to Porphyromonas gingivalis LPS. Mediators Inflamm. 2013, 407562.
Martande, S.S., Pradeep, A.R., Singh, S.P., Kumari, M., Suke, D.K., Raju, A.P., Naik, S.B., Singh, P., 2014. Periodontal health condition in patients with Alzheimer's disease. Am. J. Alzheimers. Dis. Other Demen. 29, 498–502.
McGeer, E.G., McGeer, P.L., 2010. Neuroinflammation in Alzheimer's disease and mild cognitive impairment: a field in its infancy. J. Alzheimers Dis. 19, 355–361.
Metzler-Baddeley, C., Jones, D.K., Steventon, J., Westacott, L., Aggleton, J.P., O'Sullivan, M.J., 2012. Cingulum microstructure predicts cognitive control in older age and mild cognitive impairment. J. Neurosci. 32, 17612–17619.
Nakanishi, H., Amano, T., Sastradipura, D.F., Yoshimine, Y., Tsukuba, T., Tanabe, K., Hirotsu, I., Ohono, T., Yamamoto, K., 1997. Increased expression of cathepsins E and D in neurons of the aged rat brain and their colocalization with lipofuscin and carboxy-terminal fragments of Alzheimer amyloid precursor protein. J. Neurochem. 68, 739–749.
Ni, J., Wu, Z., Peterts, C., Yamamoto, K., Qing, H., Nakanishi, H., 2015. The critical role of proteolytic relay through cathepsins B and E in the phenotypic change of microglia/macrophage. J. Neurosci. 35, 12488–12501.
Noble, J.M., Borrell, L.N., Papapanou, P.N., Elkind, M.S., Scarmeas, N., Wright, C.B., 2009. Periodontitis is associated with cognitive impairment among older adults: analysis of NHANES-III. J. Neurol. Neurosurg. Psychiatry 80, 1206–1211.
Nyberg, L., 2005. Any novelty in hippocampal formation and memory? Curr. Opin. Neurol. 18, 424–428.
Oeppen, J., Vaupel, J.W., 2002. Demography. Broken limits to life expectancy. Science 296, 1029–1031.
Okello, A., Edison, P., Archer, H.A., Turkheimer, F.E., Kennedy, J., Bullock, R., Walker, Z., Kennedy, A., Fox, N., Rossor, M., Brooks, D.J., 2009. Microglial activation and amyloid deposition in mild cognitive impairment: a PET study. Neurology 72, 56–62.
Pasternak, S.H., Callahan, J.W., Mahuran, D.J., 2004. The role of the endosomal/lysosomal system in amyloid-beta production and the pathophysiology of Alzheimer's disease: reexamining the spatial paradox from a lysosomal perspective. J. Alzheimers Dis. 6, 53–65.
Perry, V.H., 2004. The influence of systemic inflammation on inflammation in the brain: implications for chronic neurodegenerative disease. Brain Behav. Immun. 18, 407–413.
Perry, V.H., Newman, T.A., Cunningham, C., 2003. The impact of systemic infection on the progression of neurodegenerative disease. Nat. Rev. Neurosci. 4, 103–112.
Pisa, D., Alonso, R., Rábano, A., Rodal, I., Carrasco, L., 2015. Different brain regions are infected with fungi in Alzheimer's disease. Sci. Rep. 5, 15015.
Pischon, N., Heng, N., Bernimoulin, J.P., Kleber, B.M., Willich, S.N., Pischon, T., 2007. Obesity, inflammation, and periodontal disease. J. Dent. Res. 86, 400–409.
Poole, S., Singhrao, S.K., Kesavalu, L., Curtis, M.A., Crean, S., 2013. Determining the presence of periodontopathic virulence factors in short-term postmortem Alzheimer's disease brain tissue. J. Alzheimers Dis. 36, 665–677.
Puntener, U., Booth, S.G., Perry, V.H., Teeling, J.L., 2012. Long-term impact of systemic bacterial infection on the cerebral vasculature and microglia. J. Neuroinflammation 9, 146.
Pyo, J.O., Yoo, S.M., Ahn, H.H., Nah, J., Hong, S.H., Kam, T.I., Jung, S., Jung, Y.K., 2013. Overexpression of Atg5 in mice activates autophagy and extends lifespan. Nat. Commun. 4, 2300.
Rogers, J.T., Leiter, L.M., McPhee, J., Cahill, C.M., Zhan, S.S., Potter, H., Nilsson, L.N., 1999. Translation of the alzheimer amyloid precursor protein mRNA is up-regulated by interleukin-1 through 5′-untranslated region sequences. J. Biol. Chem. 274, 6421–6431.
Schrader-Fischer, G., Paganetti, P.A., 1996. Effect of alkalizing agents on the processing of the beta-amyloid precursor protein. Brain Res. 716, 91–100.
Seo, J.E., Hasan, M., Han, J.S., Kang, M.J., Jung, B.H., Kwok, S.K., Kim, H.Y., Kwon, O.S., 2015. Experimental autoimmune encephalomyelitis and age-related correlations of NADPH oxidase, MMP-9, and cell adhesion molecules: The increased disease severity and blood-brain barrier permeability in middle-aged mice. J. Neuroimmunol. 287, 43–53.
Shaftel, S.S., Griffin, W.S., O'Banion, M.K., 2008. The role of interleukin-1 in neuroinflammation and Alzheimer disease: an evolving perspective. J. Neuroinflammation 5, 7.
Sheng, J.G., Price, D.L., Koliatsos, V.E., 2003. The beta-amyloid-related proteins presenilin 1 and BACE1 are axonally transported to nerve terminals in the brain. Exp. Neurol. 184, 1053–1057.
Sparkman, N.L., Kohman, R.A., Garcia, A.K., Boehm, G.W., 2005. Peripheral lipopolysaccharide administration impairs two-way active avoidance conditioning in C57BL/6J mice. Physiol. Behav. 85, 278–288.

Streit, W.J., Mrak, R.E., Griffin, W.S., 2004. Microglia and neuroinflammation: a pathological perspective. J. Neuroinflammation 1, 14.
Su, Y., Chang, P.T., 2001. Acidic pH promotes the formation of toxic fibrils from beta-amyloid peptide. Brain Res. 893, 287–291.
Sun, L., Wu, Z., Hayashi, Y., Peters, C., Tsuda, M., Inoue, K., Nakanishi, H., 2012. Microglial cathepsin B contributes to the initiation of peripheral inflammation-induced chronic pain. J. Neurosci. 32, 11330–11342.
Terada, K., Yamada, J., Hayashi, Y., Wu, Z., Uchiyama, Y., Peters, C., Nakanishi, H., 2010. Involvement of cathepsin B in the processing and secretion of interleukin-1beta in chromogranin A-stimulated microglia. Glia 58, 114–124.
Vassar, R., Bennett, B.D., Babu-Khan, S., Kahn, S., Mendiaz, E.A., Denis, P., Teplow, D. B., Ross, S., Amarante, P., Loeloff, R., Luo, Y., Fisher, S., Fuller, J., Edenson, S., Lile, J., Jarosinski, M.A., Biere, A.L., Curran, E., Burgess, T., Louis, J.C., Collins, F., Treanor, J., Rogers, G., Citron, M., 1999. Beta-secretase cleavage of Alzheimer's amyloid precursor protein by the transmembrane aspartic protease BACE. Science 286, 735–741.
Vlad, S.C., Donald, R., Miller, D.R., Kowall, N.W., David, T., Felson, D.T., 2008. Protective effects of NSAIDs on the development of Alzheimer disease. Neurology 70, 1672–1677.
Wang, T., Lafuse, W.P., Zwilling, B.S., 2001. NFkappaB and Sp1 elements are necessary for maximal transcription of toll-like receptor 2 induced by Mycobacterium avium. J. Immunol. 167, 6924–6932.
Wang, K.C., Fan, L.W., Kaizaki, A., Pang, Y., Cai, Z., Tien, L.T., 2013. Neonatal lipopolysaccharide exposure induces long-lasting learning impairment, less anxiety-like response and hippocampal injury in adult rats. Neuroscience 234, 146–157.
Wu, Z., Nakanishi, H., 2015. Lessons from microglia aging for the link between inflammatory bone disorders and Alzheimer's disease. J. Immunol. Res. 2015, 471342.
Wu, Z., Tokuda, Y., Zhang, X.W., Nakanishi, H., 2008. Age-dependent responses of glial cells and leptomeninges during systemic inflammation. Neurobiol. Dis. 32, 543–551.
Wu, Z., Sun, L., Hashioka, S., Yu, S., Schwab, C., Okada, R., Hayashi, Y., McGeer, P.L., Nakanishi, H., 2013. Differential pathways for interleukin-1beta production activated by chromogranin A and amyloid beta in microglia. Neurobiol. Aging 34, 2715–2725.
Wyss-Coray, T., 2006. Inflammation in Alzheimer disease: driving force, bystander or beneficial response? Nat. Med. 12, 1005–1015.
Yu, W.H., Cuervo, A.M., Kumar, A., Peterhoff, C.M., Schmidt, S.D., Lee, J.H., Mohan, P. S., Mercken, M., Farmery, M.R., Tjernberg, L.O., Jiang, Y., Duff, K., Uchiyama, Y., Naslund, J., Mathews, P.M., Cataldo, A.M., Nixon, R.A., 2005. Macroautophagy–a novel Beta-amyloid peptide-generating pathway activated in Alzheimer's disease. J. Cell Biol. 171, 87–98.